Vibrational Spectroscopic and Computational Studies on Formamide Solutions of Alkali Metal Ions

Ohashi, Kazuhiko
Department of Chemistry, Faculty of Science, Kyushu University

Hikiishi, Nobutaka
Department of Chemistry, Graduate School of Science, Kyushu University

出版情報：Journal of Solution Chemistry. 49 (11), pp.1442-1457, 2020-11. Springer
バージョン：
権利関係：

Vibrational Spectroscopic and Computational Studies on Formamide Solutions of Alkali Metal Ions

Kazuhiko Ohashi [1] · Nobutaka Hikiishi [2]

Abstract Infrared (IR) spectra are measured for formamide (FA, $HCONH_2$) solutions of $Li(ClO_4)$ and $Na(ClO_4)$. Both CN stretch and CO stretch bands of FA are observed to undergo upshifts in the presence of the metal ions. Quantum chemical calculations are performed for $Li^+(FA)_n$ (n = 1–7) and $Na^+(FA)_n$ (n = 1–8) complexes in order to model the metal ions in FA solutions. In previous Raman studies of the Li^+ system, so-called chelate configuration was assumed, in which the Li^+ ion was put into the center of a ring FA dimer. However, the present calculations reveal that such a configuration is in conflict with the observed band shifts. The experimental IR spectra are reproduced by adopting appropriate isomers of $Li^+(FA)_5$ and $Li^+(FA)_6$ complexes, in which all FA molecules are coordinated to Li^+ via the O atom, with a configuration that the Li^+ ion and NH_2 group are on the same side of the CO bond. These complexes, especially $Li^+(FA)_6$, are also successful in replicating characteristic features observed in the previous Raman spectra. Similarly, an O-bound isomer of $Na^+(FA)_6$ is consistent with the experimental IR and Raman spectra of the Na^+ system. A strong coupling among the CO oscillators of FA molecules is shown to be responsible for the upshifts of the ν_{CO} modes despite the coordination via the O atom.

Keywords Formamide · Li(I) · Na(I) · Coordination modes · Vibrational frequency shifts

---

✉ Kazuhiko Ohashi

kazu@chem.kyushu-univ.jp ORCID: 0000-0002-6171-3456

[1] Department of Chemistry, Faculty of Science, Kyushu University, Motooka, Fukuoka 819-0395, Japan

[2] Department of Chemistry, Graduate School of Science, Kyushu University, Motooka, Fukuoka 819-0395, Japan

1 Introduction

Formamide (FA, $HCONH_2$) has been used as a solvent for many ionic compounds which are poorly soluble in water [1, 2]. Meanwhile, FA has been of special interest as a model compound in biochemistry [3]. FA molecule, as well as water, has an ability to solvate both cations and anions. Anions can bind to the H atom(s) of the NH_2 group of FA, whereas cations can bind to either of the O atom, the N atom, or both of FA.

A variety of experimental techniques have been applied for investigating coordination structures of metal ions in solution phase [4]. For instance, X-ray diffraction method has provided static structural information, which is believed to be one of the most reliable data. Ohtaki and Wada studied the structures of solvated Li^+ and Cl^- ions in FA by means of X-ray diffraction [5]. Meanwhile, vibrational spectroscopy has been used to investigate the coordination modes of amide molecules to the metal ion. Rao and coworkers observed a downshift of the CO stretch (ν_{CO}) frequency by infrared (IR) spectroscopy of lithium salts dissolved in various amides and suggested that the Li^+ ion binds to the O atom of amides [6]. Through Raman spectroscopy of alkali and alkaline-earth metal salts dissolved in FA, Lees et al. proposed that the metal ions bind to the O atom of FA [7]. Powell and Woollins pointed out that the downshifts of the ν_{CO} band in combination with the upshift of the CN stretch (ν_{CN}) band should be viewed as evidence for the O atom coordination [8]. Bukowska studied FA solutions of Li^+, Na^+, and Ca^{2+} by Raman and IR spectroscopy [9, 10]. When the salts were dissolved in FA, an upshifted component was newly observed in the ν_{CO} region [10], in striking contrast to the downshift of the ν_{CO} band reported in the previous studies [6, 8]. More recently, Alves and coworkers reported vibrational spectroscopic studies on FA molecules interacting with metal ions of various types. Upshifts of both ν_{CO} and ν_{CN} bands were observed in the presence of Li^+ [11, 12], Ca^{2+} [13], and Al^{3+} [14]. Bukowska [10] and also Alves [11, 12] assumed a bidentate coordination of FA via both O and N atoms in a so-called ‘chelate’ configuration. However, it is not obvious whether the bidentate coordination is consistent with the upshifts of both ν_{CO} and ν_{CN} bands or not. In our previous work, we demonstrated that bidentate $Ca^{2+}(FA)_4$ complexes are inconsistent with the

observed upshift of the ν_{CN} band [15]. We showed that the experimental Raman [13] and IR [15] spectra are reasonably reproduced by adopting $Ca^{2+}(FA)_7$ and $Ca^{2+}(FA)_8$ complexes with a monodentate coordination of all FA molecules via the O atom.

In this work, we have carried out IR spectroscopic studies on FA solutions of $M(ClO_4)$ with M = Li and Na. We have also performed quantum chemical calculations for optimizing geometries and predicting vibrational spectra of $M^+(FA)_n$ complexes as a model of M^+ in FA solutions. We aim at revealing the effects of M^+ on the vibrations of FA, in particular, the ν_{CO} and ν_{CN} modes, in order to understand coordination structures of M^+ in FA.

2 Experimental and Computational Methods

IR spectra are recorded on a Fourier transform IR spectrometer (JASCO, FT/IR-4100) using an attenuated total reflection (ATR) unit (ATR PRO670H-S) equipped with a ZnSe prism. ATR-IR spectra are obtained in the 650–4000 cm^{-1} region with a resolution of 2 cm^{-1}. $Li(ClO_4)$ and $Na(ClO_4)$ are used as a source of Li^+ and Na^+, respectively, because it is expected that the ClO_4^- anion hardly distorts the first coordination sphere of the metal ion owing to a smaller charge density on ClO_4^- than on Cl^- [13]. Lithium perchlorate (Wako, purity ≥ 98%), sodium perchlorate (Wako, purity ≥ 98%), and FA (Wako, purity ≥ 98.5%) are used as received. The salts are added to FA to prepare solutions with concentrations in the range of 1.0–4.0 $mol \cdot dm^{-3}$.

Quantum chemical calculations are carried out with Gaussian 16 program package [16]. Density functional theory (DFT) method is employed by using the Becke's three parameter hybrid functional coupled with the Lee–Yang–Parr correlation functional (B3LYP). In addition, the second-order Møller–Plesset perturbation (MP2) method is applied for selected species. 6-311+G(2df) basis sets are used for the metals and 6-31+G(d) for other atoms. Self-consistent reaction field method with Polarizable Continuum Model (PCM) is incorporated to implicitly account for extra solvent molecules surrounding the species of interest. Geometries of $Li^+(FA)_n$ (n = 1–7) and $Na^+(FA)_n$ (n = 1–8) complexes and other species in PCM are optimized without any symmetry constraints; it is confirmed that the

resulting structures have no imaginary-frequency vibration unless otherwise stated. It is generally accepted that vibrational frequencies of solvated metal complexes are better predicted by DFT than MP2 calculations [17]. Experimental values for vibrational frequencies of FA molecule in the gas phase are available in the literature [18]. Harmonic frequencies of FA in vacuum are calculated at the B3LYP/6-31+G(d) level and the scaling factor is evaluated for each fundamental vibration. The results are 0.978 for the CH scission, 0.982 for the CO stretch, and 0.973 for an average of nine fundamental vibrations above 1000 cm^{-1}. Harmonic frequencies of all vibrations, except the CH scission, of all species in PCM are scaled with the average factor of 0.973 and the CH scission frequencies are scaled with its own factor of 0.978. As an exceptional case, the CO stretch frequencies are scaled with its own factor of 0.982 in Fig. 5. The scaled frequencies and IR as well as Raman intensities are displayed as stick diagrams in the figures of this article.

3 Results and Discussion

3.1 IR Spectra of FA and FA Solutions of $Li(ClO_4)$

Figure 1a shows an ATR-IR spectrum of neat FA liquid in the 1200–1800 cm^{-1} region. Four bands with maxima around 1307, 1390, 1610, and 1673 cm^{-1} are assigned to the CN stretch (ν_{CN}), CH scission (δ_{CH}), HNH scission (δ_{HNH}), and CO stretch (ν_{CO}) bands, respectively [18, 19]. A model structure for neat FA liquid and the theoretical IR spectrum predicted for the model structure are described in section A.1 of electronic supplementary material (ESM). Figure 1b–e displays the spectra for FA solutions of $Li(ClO_4)$ at various concentrations in the range from 1.0 to 4.0 $mol \cdot dm^{-3}$. With increasing the concentration, the ν_{CN}, δ_{CH}, and ν_{CO} bands undergo gradual upshifts, while the δ_{HNH} band undergoes a gradual downshift. In the spectrum of the 4.0 $mol \cdot dm^{-3}$ solution, the ν_{CN}, δ_{CH}, δ_{HNH}, and ν_{CO} bands show maxima around 1315, 1393, 1598, and 1677 cm^{-1}, respectively. The upshifts of the ν_{CN} and ν_{CO} bands are consistent with those observed in Raman spectroscopy carried out by Alves [11, 12]. The spectra for FA solutions of $Na(ClO_4)$ are presented in section A.2 of ESM.

3.2 Effects of Adjacent Ions on the Vibrations of FA

We first explore the effects of the Li^+ ion on the vibrations of FA molecule from DFT calculations for the $Li^+(FA)_1$ complex. The results are given in section A.3 of ESM and the points are as follows. When the metal ion interacts with the O atom of FA, the ν_{CN} mode is upshifted while the ν_{CO} mode is downshifted. On the other hand, the ν_{CN} mode is downshifted while the ν_{CO} mode is upshifted, when the metal ion interacts with the N atom of FA. These results are totally consistent with the generally accepted idea about the shifts of the ν_{CN} and ν_{CO} bands of FA upon coordination to the metal ion [8].

Next we examine the interactions of $Li^+(FA)_1$ with another Li^+ and with a counter anion. The results are described in sections A.4 and A.5 of ESM and the points are as follows. Simultaneous interactions of FA with two Li^+ ions hardly lead to upshifts of both ν_{CN} and ν_{CO} modes, as demonstrated in Fig. S4 of ESM. The ν_{CO} mode never undergoes an upshift through simultaneous interactions with the Li^+ and ClO_4^- ions, as demonstrated in Fig. S5 of ESM.

3.3 Effects of FA–FA Interactions on the Vibrations of FA

Theoretical calculations are continued to examine the effects of ligand–ligand interactions on the vibrations of FA. Figure 2 illustrates the structures and theoretical IR spectra for five isomers of the $Li^+(FA)_2$ complex from DFT calculations. Isomers 2-O-i, 2-O-ii, and 2-ON* are formed by adding a second FA molecule opposite the first one in 1-O-i, 1-O-ii, and 1-ON*, respectively, with the same configuration as that of the first one. Both 2-O-i and 2-O-ii are stationary structures located at potential-energy minima. On the other hand, 2-ON* has two imaginary-frequency vibrations. In this article, an asterisk symbol attached to the structure label indicates that it is a non-stationary structure. In 2-ON*, the Li^+ ion is squeezed into the center of a ring FA dimer connected by two NH···O hydrogen bonds. The Li···O and Li···N distances are 1.834 and 2.187 Å, respectively. This structure was proposed by Rode and referred to as ‘chelate’ complex [20]. It was claimed that the hydrogen bonds in the ring dimer were remaining and Li^+ was interacting with both O and N atoms of FA in the ‘chelate’

complex [20]. Then attempts are made to find a potential-energy minimum corresponding to such a 'chelate' complex, but the geometry optimizations always end up with structures in which two FA molecules are bound to Li^+ via only the O atom. In isomers 2-O-iii and 2-O-iv, the O···Li···O angle is decreased to 110° and 105°, respectively. The smaller angle of 2-O-iv is probably due to an NH···O hydrogen bond between two FA molecules. MP2 calculations are carried out for re-optimizing the geometry and estimating the relative energy of the five isomers. Although the MP2-optimized structures are slightly different from the DFT-optimized structures, the same labels are used to identify the isomers. 2-O-iv is lowest in energy and 2-O-i, 2-O-ii, and 2-O-iii are higher by 11, 10, and 8 kJ mol^{-1}, respectively. 2-ON* lies >150 kJ mol^{-1} above 2-O-iv.

Two FA molecules are nearly equivalent to each other in 2-O-i, 2-O-ii, and 2-ON*. In each isomer, there is a coupling between the CO oscillators in FA molecules. This coupling gives rise to a splitting of the ν_{CO} modes into two normal modes; two CO oscillators vibrate out-of-phase in one mode and in-phase in the other. The frequencies of the two modes are as follows: 1674.5/1676.4 cm^{-1} for 2-O-i and 1674.2/1676.0 cm^{-1} for 2-O-ii. Only the former mode of each isomer is IR active. Overall spectral features of 2-O-i and 2-O-ii are similar to those of 1-O-i and 1-O-ii, respectively (see section A.3 of ESM). For 2-O-iv, upshifts of ν_{CN} are +39 and +52 cm^{-1} and downshifts of ν_{CO} are –15 and –6 cm^{-1}, relative to FA. For 2-O-iii, upshifts of ν_{CN} are +31 and +33 cm^{-1} and downshifts of ν_{CO} are –7 and –2 cm^{-1}. In the so-called 'chelate' structure 2-ON*, the ν_{CN} mode is located at 1300 cm^{-1}, resulting in an upshift of +34 cm^{-1}. The ν_{CO} mode (1624 cm^{-1}) undergoes a large downshift (–57 cm^{-1}) and switches position with the δ_{HNH} mode (1779 cm^{-1}). Bukowska [10] and Alves [11, 12] assumed a 'chelate' complex similar to 2-ON*. However, our calculations indicate that the ν_{CO} modes of the 'chelate' geometry is downshifted; the direction of the shift is in conflict with the results of the previous Raman [10–12] and present IR spectroscopy. Thus the 'chelate' complex of $Li^+(FA)_2$ (2-ON*) is not appropriate for a model of Li^+ in FA solutions.

3.4 Structures and IR Spectra of $Li^+(FA)_{4–7}$

Now we try to find a $Li^+(FA)_n$ complex which can be regarded as a model of Li^+ in FA solutions. As examined in sections 3.3 and A.3 of ESM, the most favorable coordination mode of FA toward Li^+ is via the O atom. Since a solvation number of 4 was reported for Li^+ in acetonitrile [21] and in acetone, *N*,*N*-dimethylformamide (DMF) and dimethylsulfoxide (DMSO) [22], we start with O-bound isomers of the $Li^+(FA)_4$ complex. Figure 3a exhibits the optimized geometry of the lowest-energy isomer of $Li^+(FA)_4$ (4-O-i) from DFT calculations. Other isomers are treated in section A.6 of ESM. In 4-O-i, four O atoms of FA adopt a tetrahedral coordination with the Li···O distances of 1.99 Å. We also examine $Li^+(FA)_n$ with n = 5 and 6, since the Li^+ ion was reported to have 5.4 FA molecules on average as nearest neighbors [5]. Figure 3b, c depicts the optimized geometries of the lowest-energy isomers of n = 5 (5-O-i) and 6 (6-O-i), respectively, from DFT calculations. Other isomers are treated in sections A.7 and A.8 of ESM. 5-O-i (Fig. 3b) is constructed by adding a fifth FA molecule under the central Li^+ ion in 4-O-i. The first four FA molecules maintain a tetrahedral coordination approximately with the Li···O distances of 1.91–2.03 Å. Two FA molecules in the tetrahedron act as H-atom donors of NH···O hydrogen bonds to the O atom of the fifth FA. As a result, the Li···O distance for the fifth FA is fairly large (3.98 Å). 6-O-i is built by squeezing a sixth FA molecule in an equatorial position of 5-O-i; six O atoms adopt an elongated octahedral coordination. The Li···O distances are 2.04–2.06 Å for FA in the equatorial positions and 3.22–3.25 Å for FA in the axial positions. All FA molecules in 4-O-i, 5-O-i, and 6-O-i are bound to Li^+ with 'cis' configuration (see section A.3 of ESM). In contrast to the $Li^+(FA)_n$ complexes with $n \leq 6$, it is not successful to find a potential-energy minimum corresponding to $Li^+(FA)_7$ with all FA molecules bound to Li^+. During the optimization processes, seven-coordinated geometries evolve to less-coordinated ones, in which only three or four FA molecules remain bound to Li^+ and the rest are put away from Li^+. A typical example is shown in Fig. 3d, where four FA molecules form the first shell around Li^+ with a distorted tetrahedral arrangement.

Figure 4b–d represents the theoretical IR spectra predicted for 4-O-i, 5-O-i, and 6-O-i,

respectively. Figure 4f displays the spectrum of the four-coordinated $Li^+(FA)_7$ (Fig. 3d). Reproduced in Fig. 4a are the experimental IR spectrum of neat FA liquid and the theoretical spectrum of the model cluster 4RL (see section A.1 of ESM). The experimental spectrum of the 4.0 mol·dm^{-3} solution is reproduced in Fig. 4e. In the theoretical spectrum of 4-O-i, the direction of the shifts of the ν_{CN}, δ_{CH}, and δ_{HNH} modes coincides with the experimental results. However, the strongest ν_{CO} mode at 1668 cm^{-1} is slightly downshifted (–4 cm^{-1}) from that of 4RL; the direction is inconsistent with the experiment. In contrast, 5-O-i has an IR active ν_{CO} mode at 1691 cm^{-1}, with an upshift of 19 cm^{-1} relative to 4RL. Similarly, 6-O-i has IR active ν_{CO} modes at 1670, 1679, and 1686 cm^{-1}, with the shifts of –2, +7, and +14 cm^{-1}, respectively. Meanwhile, most ν_{CN} modes of 5-O-i are upshifted from the averaged one of 4RL (1302 cm^{-1}), although the ν_{CN} modes of 6-O-i remain almost unshifted. Overall, the theoretical IR spectra of 5-O-i and 6-O-i are in agreement with the experimental spectrum of the 4.0 mol·dm^{-3} solution, although the spectrum of the four-coordinated $Li^+(FA)_7$ happens to be in line with the experiment as well. The most important point is that a part of the ν_{CO} modes of 5-O-i and 6-O-i undergo upshifts, in spite of the monodentate coordination via the O atom.

3.5 Raman Spectra of $Li^+(FA)_{4–6}$

Bukowska studied $Li(ClO_4)$ dissolved in deuterated FA ($HCOND_2$, FA-d_2) by Raman and IR spectroscopy [9, 10]. The ν_{CO} region of the Raman spectra is reproduced in Fig. 5e. The isotropic component of the spectrum of neat FA-d_2 liquid (solid curve) exhibits a maximum around 1640 cm^{-1} with a long tail on the high-frequency side. When the salt is dissolved (dashed curve), a new component appears around 1700 cm^{-1} and the main maximum moves to 1660 cm^{-1}. The anisotropic component shows a maximum around 1670 cm^{-1}; the position remains almost unchanged upon dissolution of the salt. Bukowska made the following assignment for the spectra of the $Li(ClO_4)$ solution. The 1660 cm^{-1} component was assigned to the non-coordinated FA-d_2 molecules. The 1700 cm^{-1} component was attributed to the CO groups, vibrating in phase, of FA-d_2 molecules coordinated to Li^+. The 1670 cm^{-1}

component was assigned to out-of-phase vibrations of FA-d_2 molecules coordinated to Li^+.

More recently, Alves studies $Li(ClO_4)$ dissolved in 1:1 mixture of FA and acetonitrile by Raman and IR spectroscopy [11, 12]. Figure 5k reproduces the ν_{CO} region of the Raman spectrum, which is decomposed into three component centered at 1685, 1700, and 1714 cm^{-1}. Alves made the following assignment. The former two components were attributed to the non-coordinated FA molecules: the 1685 cm^{-1} component to hydrogen-bonded FA molecules, while the 1700 cm^{-1} component to FA molecules free from hydrogen bonding. The 1714 cm^{-1} component was assigned to FA molecules coordinated to Li^+.

Table S1 of ESM gathers the scaled ν_{CO} frequencies, IR intensities, and Raman scattering activities of 4-O-i, 5-O-i, and 6-O-i. Each of the ν_{CO} modes is not localized on a CO group of a particular FA molecule in the complexes, but is a normal mode vibration delocalized over all FA molecules. The highest-frequency mode of each complex involves in-phase motions of the CO groups of all FA molecules. The IR intensity of this mode of 4-O-i and 6-O-i is almost zero because of the symmetry of the structures. On the other hand, the Raman activity of this in-phase mode is large. The other modes involve out-of-phase motions of the CO groups. In 4-O-i and 6-O-i, those modes with large IR intensities have small Raman activities. It should be noted that the lowest-frequency mode of each complex has a large Raman activity.

Let us take a look at the spectrum reported by Alves first. Figure 5g–j shows the theoretical Raman spectra of 4-O-i, 5-O-i, 6-O-i, and 6-O-ii (Fig. S8b of ESM), respectively. Figure 5m, l represents the spectra of the FA monomer and 4RL, respectively. Here, the harmonic frequencies are scaled with a factor of 0.982, which is an own scaling factor for the ν_{CO} mode. The use of this factor brings the theoretical ν_{CO} frequencies into better agreement with the experimental ones. A comparison of the spectra between the FA monomer and 4RL indicates that the ν_{CO} modes of hydrogen-bonded FA molecules are located at frequencies lower than that of the FA monomer (1696 cm^{-1}). In this sense, the assignment of the 1685 and 1700 cm^{-1} components made by Alves is plausible. The highest-frequency modes of 5-O-i, 6-O-i, and 6-O-ii are located at frequencies higher than the mode of the FA monomer.

Accordingly, it is likely that these complexes contribute to the 1714 cm^{-1} component. On the other hand, 5-O-i, 6-O-i, and 6-O-ii have Raman active modes also in the 1678–1686 cm^{-1} regions; these lowest-frequency modes are likely to contribute to the 1685 cm^{-1} component. Indeed, the intensity of the 1685 cm^{-1} component might be too large in the spectrum of the concentrated solution, if only the non-coordinated FA molecules would contribute to this component. Therefore, we are opposed to Alves's assignment of the 1685 cm^{-1} component solely to the non-coordinated FA molecules.

Next we turn to the spectra reported by Bukowska. The computational data for the normal FA species are used to retrieve the corresponding data for the FA-d_2 species. Figure 5a–d exhibits the theoretical Raman spectra of 4-O-i-d_2, 5-O-i-d_2, 6-O-i-d_2, and 6-O-ii-d_2 (Fig. S8b of ESM), respectively. The spectrum of 4RL-d_2 is depicted in Fig. 5f. The 1643 cm^{-1} mode of 4RL-d_2 (Fig. 5f) contributes to the 1640 cm^{-1} maximum in the isotropic component of neat FA-d_2 liquid (Fig. 5e), while the 1679 cm^{-1} mode contributes to the high-frequency tail. For 5-O-i-d_2 and 6-O-i-d_2, the lowest- and highest-frequency modes have large Raman activities (Fig. 5b, c), which are consistent with the bimodal profile of the isotropic component of the $Li(ClO_4)$ solution. In particular, the 1653 and 1700 cm^{-1} modes of 6-O-i-d_2 nicely match the 1660 and 1700 cm^{-1} maxima of the experimental spectrum, respectively. Meanwhile, the spacing may be too small between the 1671 and 1683 cm^{-1} modes of 6-O-ii-d_2. As already noted, Bukowska assigned the 1660 cm^{-1} component solely to the non-coordinated FA-d_2 molecules. However, our interpretation is that the 1660 cm^{-1} component originates not only from the non-coordinated but also from the coordinated FA-d_2 molecules, as in the case of the 1685 cm^{-1} component of the Alves's spectrum. In common with the IR spectra, 5-O-i and more preferably 6-O-i are successful in replicating the characteristic features observed in the Raman spectra.

3.6 Structures and IR/Raman Spectra of $Na^+(FA)_{5–8}$

Now we attempt to find a $Na^+(FA)_n$ complex as a model of Na^+ in FA solutions. We focus on O-bound isomers, as in the case of Li^+. Since molecular dynamics (MD) simulations

provided coordination numbers of 5–6 for Na^+ in FA [23], we start with the $Na^+(FA)_5$ complex. Figure 6a, b illustrates the optimized geometries of the lowest-energy isomers of $Na^+(FA)_5$ (5-O-I) and $Na^+(FA)_6$ (6-O-I), respectively, from DFT calculations. Hereafter, Roman numerals in upper case are used to label isomers of the Na^+ complexes. 5-O-I is constructed by adding a fifth FA molecule over the central Na^+ ion in a square-planar isomer of $Na^+(FA)_4$ which is similar to 4-O-ii of $Li^+(FA)_4$. In 5-O-I, five O atoms of FA are arranged to form a square-pyramid with the Na···O distances of 2.37–2.50 Å. 6-O-I is built by adding a sixth FA molecule under the Na^+ ion in 5-O-I. Six O atoms adopt an octahedral coordination with the Na···O distances of 2.42–2.50 Å. Other isomers of $Na^+(FA)_6$ are treated in section A.9 of ESM. We make a comparison of the geometries between 6-O-i (Li^+) and 6-O-I (Na^+) in section A.10 of ESM. Figure 6c, d displays a stable structure of $Na^+(FA)_7$ (7-O-I), which is similar to the lowest-energy isomer of $Ca^{2+}(FA)_7$ [15]. Such a seven-coordinated isomer is not the lowest-energy one; an initial geometry similar to 7-O-I, for instance, evolves to a lower-energy isomer 7-O-II (Fig. 6e, f) during the optimization process. In 7-O-II, only six FA molecules remain bound to Na^+ and the seventh one is hydrogen-bonded to the first-shell molecules. Six O atoms of the first-shell FA adopt an octahedral coordination with the Na···O distances of 2.43–2.49 Å, while the Na···O distance is 4.80 Å for the second-shell FA. It is not successful to find a potential-energy minimum of $Na^+(FA)_8$ corresponding to the lowest-energy isomer of $Ca^{2+}(FA)_8$ [15]. The optimization processes end up with structures in which only four to six FA molecules, depending on the initial geometry, remain bound to Na^+ and the rest are located away from Na^+.

Figure 7b–e shows the theoretical IR spectra predicted for 5-O-I, 6-O-I, 7-O-I, and 7-O-II, respectively. Reproduced in Fig. 7a are the experimental IR spectrum of neat FA liquid and the theoretical spectrum of 4RL. The experimental spectrum of the 3.0 mol·dm^{-3} solution is reproduced in Fig. 7f. We may rule out 7-O-I, because the averaged ν_{CN} frequency (1298 cm^{-1}) is lower than that of 4RL (1302 cm^{-1}) and the shifts of the ν_{CO} modes are too large. In contrast, the strongest ν_{CO} mode of 5-O-I at 1676 cm^{-1} is moderately upshifted (+4 cm^{-1}) from that of 4RL. Similarly, 6-O-I has IR active ν_{CO} modes at 1672,

1675, and 1680 cm^{-1}, with the shifts of 0, +3, and +8 cm^{-1}, respectively. The strongest ν_{CO} mode of 7-O-II at 1676 cm^{-1} is upshifted (+4 cm^{-1}) from that of 4RL. The averaged ν_{CN} frequencies of 5-O-I, 6-O-I, and 7-O-II are upshifted from that of 4RL. These spectral features are consistent with the experimental observation.

Bukowska reported the ν_{CO} region of the Raman spectra for FA-d_2 solutions of $Na(ClO_4)$ [10]. In section A.11 of ESM, the experimental Raman spectrum is compared with the theoretical spectra predicted for the model complexes composed of FA-d_2 molecules. The comparison reveals that the spectrum of 6-O-I best replicates the experimental spectrum, although the coexistence of other complexes may improve the agreement with the experiment.

Overall, 6-O-I is most successful in reproducing the experimental IR and Raman spectra of the concentrated solutions.

3.7 Direction of the Shift of the ν_{CO} Band

Let us consider the direction of the shift of the ν_{CO} band along the same lines as our previous work for the Ca^{2+} system [15]. Both ν_{CO} and ν_{CN} bands of FA are upshifted under the influence of Li^+. The upshift of the ν_{CN} band is expected, but the upshift of the ν_{CO} band is unexpected for the O-bound complexes [8]. Figure 8 represents a diagram of the vibrational energy levels for selected species, which helps us understand the upshift of the ν_{CO} band. As demonstrated in section A.3 of ESM, the ν_{CO} mode is downshifted by –6 cm^{-1} for both 1-O-i and 1-O-ii. This means that a one-to-one interaction between the Li^+ ion and the O atom of FA in $Li^+(FA)_1$ leads to the downshift; the direction is consistent with the expectation. As described in section 3.3, there is a coupling between the CO oscillators in $Li^+(FA)_2$. The coupling gives rise to a splitting of the ν_{CO} modes; the width of the splitting is denoted by Δ hereafter. The magnitude of the splitting is Δ = 1.9 and 1.8 cm^{-1} for 2-O-i and 2-O-ii, respectively. As listed in Table S1 of ESM, Δ = 32 cm^{-1} for 6-O-i, which is much larger than the magnitude of the downshift due to the one-to-one interaction between Li^+ and FA in 1-O-i and 1-O-ii. It should be noted that the interactions among the transition dipoles of the CO stretches are especially large, since the magnitude of the splitting for other modes of 6-O-i is

as follows: $\Delta(\nu_{CN}) = 16$ cm^{-1}, $\Delta(\delta_{CH}) = 12$ cm^{-1}, and $\Delta(\delta_{HNH}) = 15$ cm^{-1}. The interactions among the CO oscillators, and hence the intermolecular interactions among FA molecules in the first shell, surpass the interactions between Li^+ and FA. As a result, two out of six ν_{CO} modes of 6-O-i are upshifted from the highest-frequency mode of 4RL, despite the supposed downshifts due to the $Li^+\cdots$FA interactions.

The magnitude of the splitting is $\Delta = 14$ cm^{-1} for the Na^+ complex 6-O-I, which is much smaller than that of the Li^+ complex 6-O-i (32 cm^{-1}). Influence of the metal ion on the vibration of FA is smaller for Na^+ than for Li^+, probably because the charge density on the metal ion is smaller in Na^+ than in Li^+.

3.8 Coordination Structures of Li^+ and Na^+ in FA

As already noted in section 3.5, Bukowska interpreted that the ν_{CO} band in the Raman spectra consists of three components centered at 1660, 1670, and 1700 cm^{-1} [10]. He attributed the 1660 cm^{-1} component to the non-coordinated FA molecules. Since this component has an appreciable intensity even in the concentrated solutions, Bukowska thought that a considerable amount of the non-coordinated FA molecules would still remain in the solutions. He offered two possible explanations for the observation. The first was a two-site interaction model, in which one FA molecule was interacting with two Li^+ ions at the same time. In the second explanation, assumed was a $Li^+(FA)_2$ complex with a 'chelate' configuration similar to 2-ON*, after ab initio calculations performed by Rode [20].

In section 3.5, we propose that the 1660 cm^{-1} component originates not only from the non-coordinated FA molecules but also from the coordinated FA molecules. If this is the case, the appreciable intensity of the 1660 cm^{-1} component does not necessarily indicate a large amount of the non-complexed FA molecules in the concentrated solutions. Then, it is not necessary to invoke either the two-site interaction model or the $Li^+(FA)_2$ complex with a 'chelate' configuration. Actually, we demonstrate in section A.3 of ESM that the two-site interaction model is inconsistent with the experimental observation.

Later, Alves observed upshifts of both ν_{CN} and ν_{CO} bands in the Raman spectrum and

assumed a bidentate coordination of FA to Li^+ with the formation of a 'chelate' ring [12], in keeping with the explanation made by Bukowska [10]. As described in section 3.3, however, such a 'chelate' geometry is not stable for $Li^+(FA)_2$ from DFT and MP2 calculations. Moreover, the ν_{CO} modes of 'chelate' geometries are downshifted; the direction is in conflict with the results of the previous and present experiments.

As demonstrated in sections 3.4 and 3.5, successful models of Li^+ in FA solutions are $Li^+(FA)_5$ and more preferably $Li^+(FA)_6$, where all FA molecules are coordinated to Li^+ via the O atom. Nevertheless, we may discard the O-bound isomers with all FA molecules in 'trans' configuration (4-O-iii, 4-O-iv, 5-O-iii, 5-O-iv, 6-O-iv, and 6-O-v), because the ν_{CN} modes of these isomers are downshifted from the average value of 4RL (Fig. S6–9 of ESM), in spite of the monodentate coordination via the O atom. Among the complexes with all FA molecules in 'cis' configuration, 4-O-i may not be probable, because the strongest ν_{CO} mode is downshifted from that of 4RL. 6-O-ii may not be probable, because the spacing is too small between the 1671 and 1683 cm^{-1} modes of 6-O-ii-d_2. After all, 5-O-i and 6-O-i remain to be candidates, the theoretical spectra of which are in accord with the experimental observation.

Ohtaki and Wada investigated structures of solvated Li^+ and Cl^- in FA by means of X-ray diffraction [5]. They reported that the average coordination number of Li^+ with FA is 5.4 ± 0.3 with the Li···O distances of 2.24 ± 0.02 Å [5]. According to re-optimization of the geometries at the MP2 level of theory, we find that the average Li···O distances are 2.32 Å for 5-O-i and 2.38 Å for 6-O-i, which are longer than the experimental value by 0.08 and 0.14 Å, respectively. The agreement with the experiment will be improved by explicitly accounting for solvent molecules in outer shells. In section A.12 of ESM, we describe influence of solvent molecules in the second shell on the vibrational spectra of the model complexes. The fractional value (5.4) for the coordination number was explained in terms of the existence of solvated Li^+ with various numbers of FA molecules [5]. The value of 5.4 is consistent with the coexistence of the five- and six-coordinated Li^+ complexes (5-O-i and 6-O-i). In addition, the coordination structure of Li^+ may be non-rigid in real solutions and FA molecules may easily come in and get out from the first solvation shell. The coordination

number of 5.4 in FA is larger than the number of 4.3 in water [4], despite the larger molecular size of FA. A plausible explanation for this observation is given in section A.10 of ESM.

As demonstrated in sections 3.6 and A.10 of ESM, most successful model of Na^+ in FA solutions is $Na^+(FA)_6$. Six-coordinated isomers of $Na^+(FA)_7$ are lower in energy than seven-coordinated isomers. As in the case of the Li^+ system, we may discard the O-bound isomers of $Na^+(FA)_6$ with all FA molecules in 'trans' configuration (6-O-IV, and 6-O-V), because the ν_{CN} modes of these isomers are downshifted from the average value of 4RL (Fig. S10, 11 of ESM). Among the complexes with all FA molecules in 'cis' configuration, 6-O-II and 6-O-III may be less probable, because the strongest ν_{CO} modes are almost unshifted from that of 4RL. After all, 6-O-I turns out to be the most appropriate model, the theoretical spectra of which are in best agreement with the experimental results.

Finter and Hertz carried out Nuclear Magnetic Resonance (NMR) relaxation study on solvation structures of Na^+ and I^- in FA [24]. They determined the ion–solvent configuration in the solvation shell, using the closest distances of approach between the interacting nuclei. By setting the Na···O distance to be 2.4 Å, they derived that the closest distance of approach between Na^+ and the formyl H of FA is 4.4 Å and the Na···O–C angle is approximately 150°. The proposed Na^+–FA configuration is quite similar to the $Na^+(FA)_1$ complex with 'cis' configuration (1-O-II, not shown), which corresponds to 1-O-ii of $Li^+(FA)_1$. In 1-O-II, the Na···O distance is 2.30 Å, the Na···H(formyl) distance is 4.31 Å, and the Na···O–C angle is 140°. We demonstrate that the model $Na^+(FA)_n$ complexes should contain FA molecules in 'cis' configuration, in order to reproduce the upshifts of the ν_{CN} band. This point is totally consistent with the Na^+–FA configuration derived by Finter and Hertz [24]. For a comparison with the NMR results, the average values for the structural parameters of 6-O-I are as follows: 2.45 Å for the Na···O distance, 4.38 Å for the Na···H(formyl) distance, and 130° for the Na···O–C angle.

MD simulations were applied to solvation of Na^+ in FA and in FA/water mixtures [23, 25]. One of the recent works provided coordination numbers of 5–6 for Na^+ in FA [23]. In a snapshot of Na^+ and eight FA molecules presented in ref. [23], the Na^+ ion is coordinated by

six FA molecules with ‘cis’ configuration. The coordination numbers and configuration provided from the MD simulations are coincide with the static structure (6-O-I) proposed in this work.

4 Conclusions

Vibrational spectroscopy has been used to investigate the coordination modes of amide molecules to the metal ion [6–15]. So far, it has been thought that, for amide molecules, a decrease in the ν_{CO} frequency and an increase in the ν_{CN} frequency are evidence for the O atom coordination [8]. However, upshifts of both ν_{CO} and ν_{CN} bands were observed for FA solutions of alkali and alkaline-earth metal salts [11–14]. In order to explain the unusual observation, a bidentate coordination via both O and N atoms was assumed, instead of the usual monodentate coordination via the O atom.

We demonstrate in this work that the ν_{CN} modes of the bidentate $Li^+(FA)_2$ complex with a ‘chelate’ configuration undergo downshifts, which are inconsistent with the experimental observation. Instead, O-bound isomers of the $Li^+(FA)_5$ and $Li^+(FA)_6$ complexes with appropriate configurations are found to be successful in reproducing the experimental IR and Raman [10–12] spectra, as in the case of the Ca^{2+} system [15]. Similarly, the experimental IR and Raman [10] spectra of the Na^+ system are replicated by adopting an O-bound $Na^+(FA)_6$ complex with appropriate configuration. The interactions among the CO oscillators in $Li^+(FA)_6$ and $Na^+(FA)_6$ give rise to splitting of the ν_{CO} modes. The magnitude of the splitting is larger than that of the downshift supposed to occur due to the one-to-one interactions between the metal ion and the O atom of FA. As a result, a part of the ν_{CO} modes are shifted to frequencies higher than those of neat FA liquid.

It has been generally accepted that the metal–ligand interactions solely determine the direction of the frequency shifts of the intramolecular vibrations of the ligands. However, for the ν_{CO} modes of FA, the intermolecular interactions among the ligands play a dominant role in determining the direction of the shift.

Acknowledgments The computations are carried out by using the computer facilities at Research Institute for Information Technology, Kyushu University. We thank Ryotaro Wakimoto for his help in measuring the IR spectra for the Li^+ system.

References

1. Wypych, G. (ed.): Handbook of Solvents, vol. 1, 3rd edn. ChemTec Publishing, Tronto (2019)
2. Ohtaki, H., Funaki, A., Rode, B.M., Reibnegger, G.J.: The Structure of Liquid Formamide Studied by Means of X-ray Diffraction and ab Initio LCGO-MO-SCF Calculations. Bull. Chem. Soc. Jpn. **56**, 2116–2121 (1983)
3. Lippard, S.J., Berg, J.M.: Principles of Bioinorganic Chemistry. Univ. Science Books, California (1994)
4. Ohtaki, H., Radnai, T.: Structure and Dynamics of Hydrated Ions. Chem. Rev. **93**, 1157–1204 (1993)
5. Ohtaki, H., Wada, H.: Structure of Solvated Lithium and Chloride Ions in Formamide. J. Sol. Chem. **14**, 209–219 (1985)
6. Balasubramanian, D., Goel, A., Rao, C.N.R.: Interaction of Amides with Lithium Ion. Chem. Phys. Lett. **17**, 482–485 (1972)
7. Lees, A.J., Straugham, B.P., Gardiner, D.J.: Electrolyte–Formamide Interactions Studied by Raman Spectroscopy. J. Mol. Struct. **71**, 61–70 (1981)
8. Powell, D.B., Woollins, A.: Vibrational Spectra of Metal Formamide Complexes. Spectrochim. Acta A **41**, 1023–1033 (1985)
9. Bukowska, J., Miaskiewicz, K.: Infrared, Raman, and CNDO Studies of the Effect of Ions on the Electron Density Distribution in Formamide. J. Mol. Struct. **74**, 1–10 (1981)
10. Bukowska, J.: Raman and Infrared Studies of Interactions between Amides and Ions. J. Mol. Struct. **98**, 1–10 (1983)
11. Alves, W.A.: Vibrational Spectroscopic and Conductimetric Studies of Lithium Battery

Electrolyte Solutions. Vib. Spectrosc. **44**, 197–200 (2007)

12. Alves, W.A.: Vibrational Spectroscopic Characterization of Stable Solvates in the $LiClO_4$/Formamide:Acetonitrile System. J. Mol. Struct. **829**, 37–43 (2007)
13. Silva, E.F., Alves, W.A.: Vibrational Study on the Solvates Formed during Interactions of Amide with Alkaline Earth Metal Ions. Vib. Spectrosc. **62**, 264–267 (2012)
14. Campos, T.B.C., Silva, E.F., Alves, W.A.: A Raman Study on the Coordination Sites and Stability of the $[Al(formamide)_5]Cl_3$ Complex. Vib. Spectrosc. **65**, 24–27 (2013)
15. Ohashi, K., Hikiishi, N., Takeshita, H.: Infrared Spectroscopic and Computational Studies on Formamide Solutions of Ca^{2+}. Vibrational Frequencies of Formamide and Modes of Coordination to Ca^{2+}. Spectrochim. Acta A **206**, 112–119 (2019)
16. Frisch, M.J., et al.: Gaussian 16, Revision A.03, Gaussian, Inc., Wallingford CT (2016)
17. Lee, E.C., Lee, H.M., Tarakeshwar, P., Kim, K.S.: Structures, Energies, and Spectra of Aqua-Silver (I) Complexes. J. Chem. Phys. **119**, 7725–7736 (2003)
18. McNaughton, D., Evans, C.J., Lane, S., Nielsen, C.J.: The High-Resolution FTIR Far-Infrared Spectrum of Formamide. J. Mol. Spectrosc. **193**, 104–117 (1999)
19. Suzuki, I.: Infrared Spectra and Normal Vibrations of Formamide; $HCONH_2$, $HCOND_2$, $DCONH_2$ and $DCOND_2$. Bull. Chem. Soc. Jpn. **33**, 1359–1365 (1960)
20. Rode, B.M.: Quantum Chemical Aspects of the Chelate Effect in Complexes. Chem. Phys. Lett. **26**, 350–355 (1974)
21. Xuan, X., Zhang, H., Wang, J., Wang, H.: Vibrational Spectroscopic and Density Functional Studies on Ion Solvation and Association of Lithium Tetrafluorobrate in Acetonitrile. J. Phys. Chem. A **108**, 7513–7521 (2004)
22. Alía, J.M., Edwards, H.G.M.: Ion Solvation and Ion Association in Lithium Trifluoromethanesulfonate Solutions in Three Aprotic Solvents. An FT-Raman Spectroscopic Study. Vib. Spectrosc. **24**, 185–200 (2000)
23. Bostick, D.L., Brooks III, C.L.: Selective Complexation of K^+ and Na^+ in Simple Polarizable Ion–Ligating Systems. J. Am. Chem. Soc. **132**, 13185–13187 (2010)
24. Finter, C.K., Hertz, H.G.: NMR Relaxation Study of I^- and Na^+ Solvation Structure in

Formamide (FA) and Preferential Solvation of These Ions in the Mixture FA/H_2O. Z. Phys. Chem. N. F. **148**, 75–96 (1986)

25. Puhovski, Y.P., Rode, B.M.: Molecular Dynamics Simulations of Na^+ and $C1^-$ Ions Solvation in Aqueous Mixtures of Formamide. Chem. Phys. **222**, 43–57 (1997)

Figure Captions

Fig. 1 ATR-IR spectra in the 1200–1800 cm^{-1} region: (a) neat FA liquid, (b) 1.0, (c) 2.0, (d) 3.0, and (e) 4.0 $mol \cdot dm^{-3}$ solutions of $Li(ClO_4)$ in FA at ambient temperature. Transmittance is plotted upside down and amplitude of all spectra is normalized to have the same maximum height. The maximum intensity around 1690 cm^{-1} corresponds to a transmittance of ≈ 0.5. Dashed lines indicate the positions of band maxima in the spectrum of neat FA liquid

Fig. 2 Structures and theoretical IR spectra of (a) FA monomer and $Li^+(FA)_2$: (b) 2-O-i, (c) 2-O-ii, (d) 2-O-iii, (e) 2-O-iv, and (f) 2-ON*

Fig. 3 Lowest-energy structures of $Li^+(FA)_n$ (n = 4–6): (a) 4-O-i, (b) 5-O-i, and (c) 6-O-i. (d) Optimized structure of four-coordinated $Li^+(FA)_7$

Fig. 4 Theoretical IR spectra of (a) 4RL and $Li^+(FA)_n$ (n = 4–6): (b) 4-O-i, (c) 5-O-i, (c) 6-O-i, and (f) four-coordinated $Li^+(FA)_7$. Dashed curves in (a) and (e) stand for experimental IR spectra of neat FA liquid and 4.0 $mol \cdot dm^{-3}$ solution of $Li(ClO_4)$ in FA, respectively. Amplitude of the spectra in the 1200–1500 cm^{-1} region is magnified by a factor of 3

Fig. 5 Theoretical Raman spectra of (a) 4-O-i-d_2, (b) 5-O-i-d_2, (c) 6-O-i-d_2, (d) 6-O-ii-d_2, and (f) 4RL-d_2. (e) Isotropic and anisotropic components of experimental Raman spectra for neat FA-d_2 liquid (solid curves) and 3.8 $mol \cdot dm^{-3}$ solution of $Li(ClO_4)$ in FA-d_2 (dashed curves) taken from the literature [10]. Theoretical Raman spectra of (g) 4-O-i, (h) 5-O-i, (i) 6-O-i, (j) 6-O-ii, (l) 4RL, and (m) FA monomer. (k) Experimental Raman spectrum for 5.0 $mol \cdot dm^{-3}$ solution of $Li(ClO_4)$ in 1:1 mixture of FA and acetonitrile taken from the literature [12]

Fig. 6 Lowest-energy structures of $Na^+(FA)_n$ (n = 5 and 6): (a) 5-O-I and (b) 6-O-I. (c ,d) Top and side views of seven-coordinated $Na^+(FA)_7$ (7-O-I). (e ,f) Top and side views of six-coordinated $Na^+(FA)_7$ (7-O-II)

Fig. 7 Theoretical IR spectra of (a) 4RL and $Na^+(FA)_n$ (n = 5–7): (b) 5-O-I, (c) 6-O-I, (d) 7-O-I, and (e) 7-O-II. Dashed curves in (a) and (f) stand for experimental IR spectra of neat FA liquid and 3.0 $mol \cdot dm^{-3}$ solution of $Na(ClO_4)$ in FA, respectively. Amplitude of the spectra in the 1200–1500 cm^{-1} region is magnified by a factor of 3

Fig. 8 Diagram of vibrational energy levels for FA monomer, $Li^+(FA)_n$ (n = 1, 2, and 6), $(FA)_4$, and $Na^+(FA)_6$. Labels for the species are indicated at the bottom

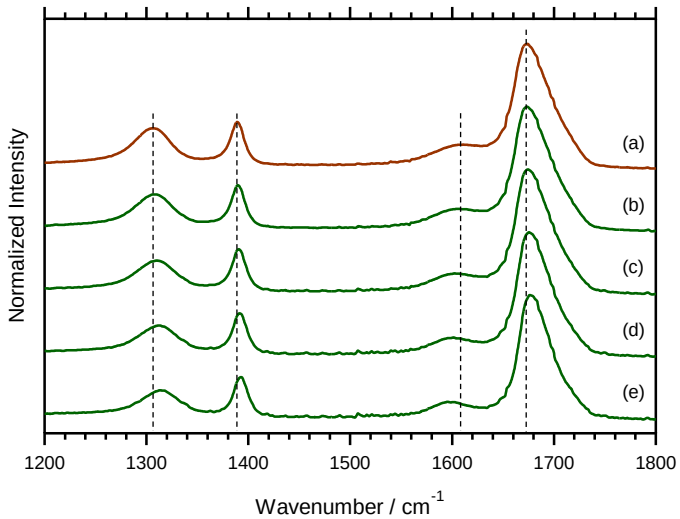

Fig. 1 Ohashi et al.

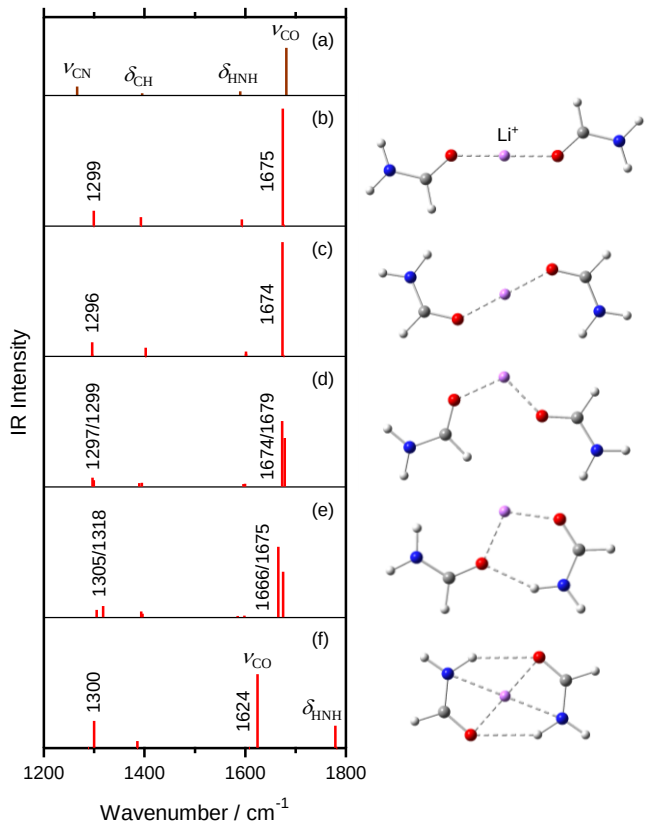

Fig. 2 Ohashi et al.

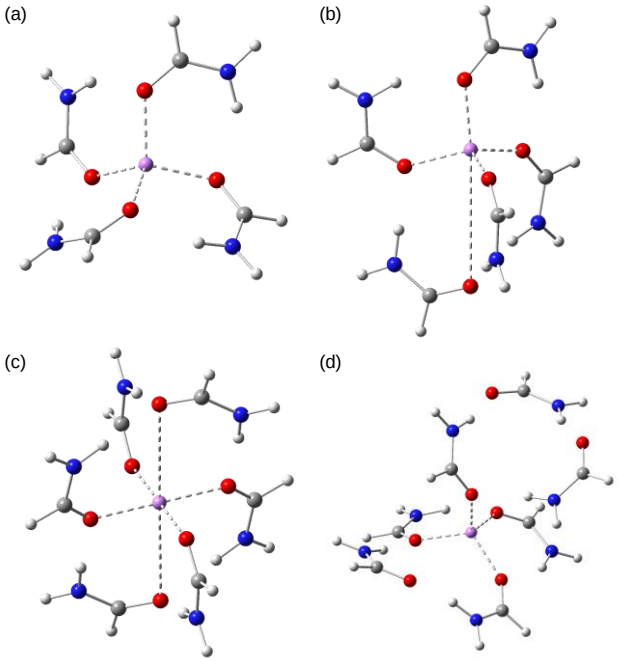

Fig. 3 Ohashi et al.

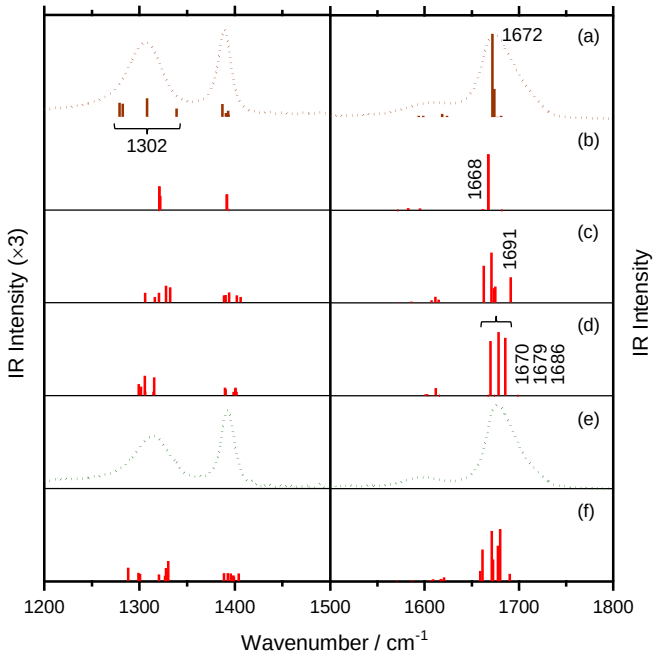

Fig. 4 Ohashi et al.

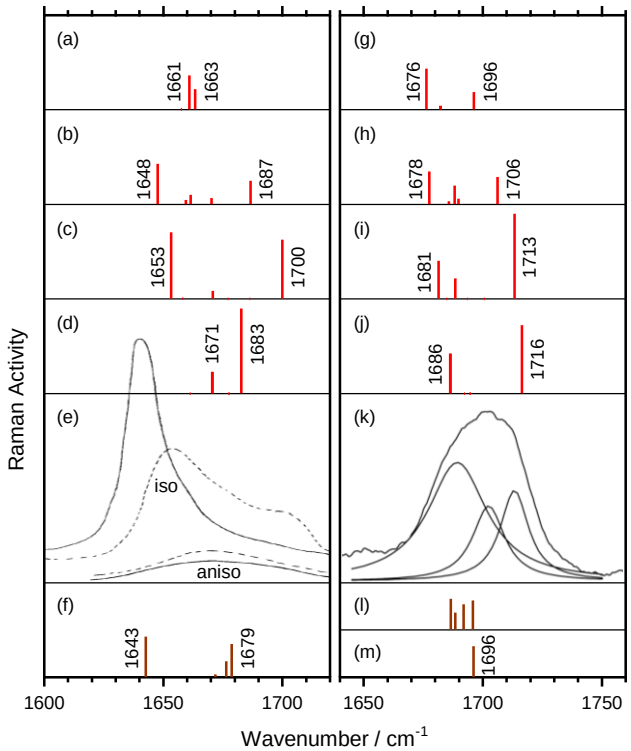

Fig. 5 Ohashi et al.

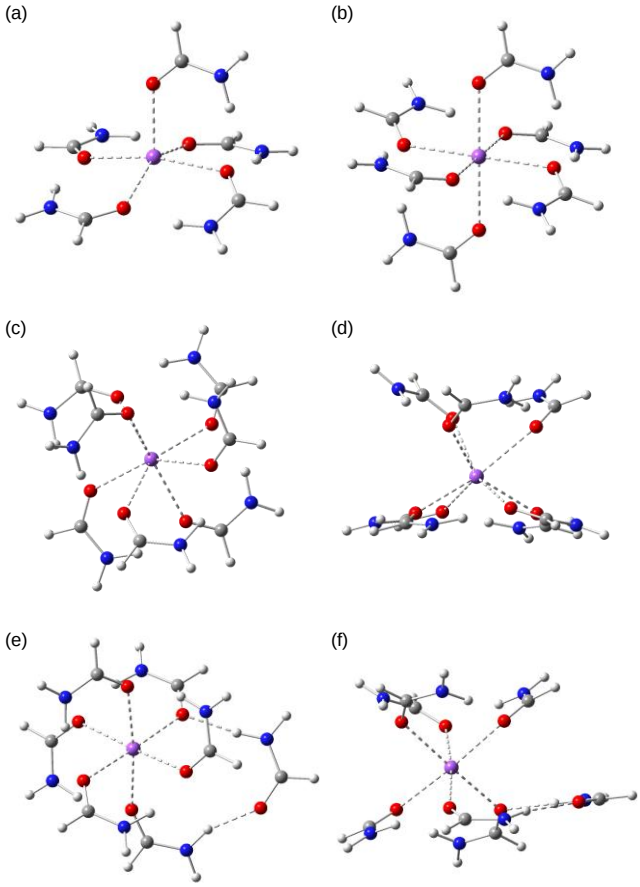

Fig. 6 Ohashi et al.

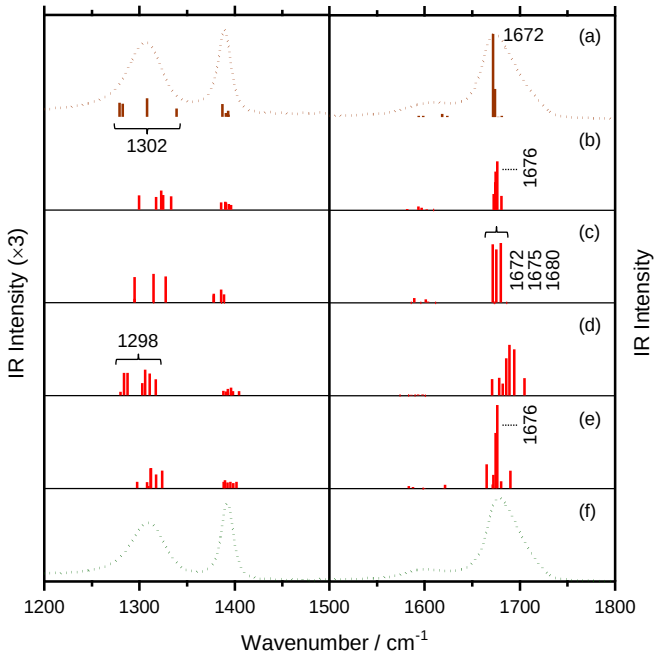

Fig. 7 Ohashi et al.

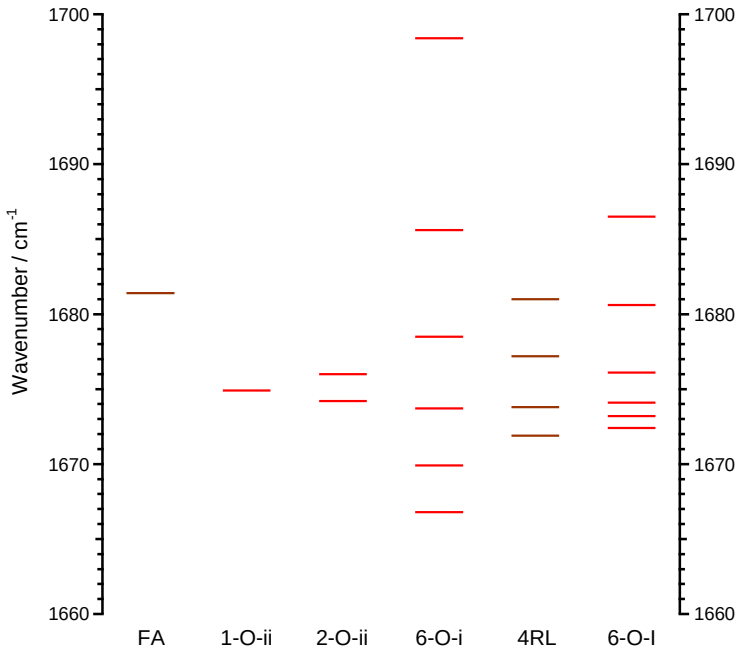

Fig. 8 Ohashi et al.